remote sensing

MDPI

Article

Predicting Dynamics of the Potential Breeding Habitat of *Larus saundersi* by MaxEnt Model under Changing Land-Use Conditions in Wetland Nature Reserve of Liaohe Estuary, China

Yu Chang [1], Chang Chang [1,2], Yuxiang Li [3], Miao Liu [1,*], Jiujun Lv [4] and Yuanman Hu [1]

[1] Institute of Applied Ecology, Chinese Academy of Sciences, Shenyang 110016, China; changyu@iae.ac.cn (Y.C.); changchang20@mails.ucas.ac.cn (C.C.); huym@iae.ac.cn (Y.H.)
[2] University of Chinese Academy of Sciences, Beijing 100049, China
[3] The Panjin Service Center for Forest and Wetland Conservation, Panjin 124010, China; liyuxiang1966@163.com
[4] Liaoning Science and Technology Center for Ecological and Environmental Protection, Shenyang 110161, China; lvjiujun@163.com
* Correspondence: lium@iae.ac.cn

Abstract: Identifying waterfowl habitat suitability under changing environments, especially land-use change, is crucial to make waterfowl habitat conservation planning. We took Wetland Nature Reserve of Liaohe Estuary, the largest breeding area of Saunders's Gulls (*Larus saundersi*) in the world, as our study area, generated land-use-type maps through interpretation of satellite images from four different years (1988, 2000, 2009, 2017), and predicted the potential breeding habitat of Saunders's Gulls by MaxEnt model based on the land-use map, along with other environmental variables (NDVI, distance to roads and artificial facilities, distance to rivers and water bodies, DEM and distance to shoreline) for the four years, respectively. The models were evaluated using the area under the curve (AUC). We analyzed the changes of the breeding habitat from 1988 to 2017 and utilized RDA to explore the relationships among the changes of suitable habitat of *Larus saundersi* and the dynamics of land uses. Our results showed that the most suitable habitat decreased by 1286.46 ha during 1988-2009 and increased by 363.51 ha from 2009 to 2017. The suitable habitat decreased by 582.48 ha from 1988 to 2009 and then increased to 1848.96 ha in 2017, while the unsuitable habitat increased by 2793.87 ha during 1988–2009 and then decreased by 178.83 ha from 2009 to 2017. We also found that land use, distance to the coastline, distance to artificial facilities, distance to rivers, distance to roads, and NDVI had certain degrees of impact on the *Larus saundersi* distribution. The contribution of land use ranged from 16.4% to 40.3%, distance to coastline from 34.7% to 48.0%, distance to artificial facilities from 5.9% to 11.1%, distance to rivers from 5.5% to 11.0%, distance to roads from 3.9% to 12.5%, and NDVI from 0.3% to 6.3%. The change in suitable habitat of *Larus saundersi* has a positive relationship with the change of seepweed marsh. Human-induced changes in seepweed marsh and coastline position are the main factors influencing the potential breeding habitat of Saunders's Gulls. We suggest strict conservation of seepweed marsh and implementation of habitat management practices to better protect Saunders' Gull's breeding habitat.

Keywords: breeding habitat; land use; MaxEnt model; Saunders's gull

Citation: Chang, Y.; Chang, C.; Li, Y.; Liu, M.; Lv, J.; Hu, Y. Predicting Dynamics of the Potential Breeding Habitat of *Larus saundersi* by MaxEnt Model under Changing Land-Use Conditions in Wetland Nature Reserve of Liaohe Estuary, China. *Remote Sens.* **2022**, *14*, 552. https://doi.org/10.3390/rs14030552

Academic Editors: Alfredo Huete and Parth Sarathi Roy

Received: 3 December 2021
Accepted: 20 January 2022
Published: 24 January 2022

1. Introduction

Wetlands are large carbon sinks [1–3] that can be used for climate mitigation, maintaining high biodiversity [4], and they are crucial habitats for various waterbird species [5,6]. However, to meet land requirements for social and economic development, wetland loss and degradation are common phenomena in coastal regions worldwide. Research shows that at least 33% of global wetlands have been lost [7]. The loss of these wetlands has seriously threatened the habitat of waterfowl [8] and biodiversity [9].

The loss of wetlands could be attributed to drought [10,11], urban growth and industrial development [12–14], climatic variability [15,16], sea-level rise [17], coastal erosion [18], etc. However, human-induced land-use changes are the key driver of wetland loss [19–21], especially agricultural activities [22–25], all over the world. Therefore, exploring waterfowl habitat suitability under changing land use could identify priority sites [26] to better plan waterfowl habitat conservation [27].

Saunders's gulls (*Larus saundersi*), which mainly breed along the east coast of China, are recognized as "vulnerable" by the IUCN [28]. The Wetland Nature Reserve of the Liaohe Estuary (WNRLE) is the largest breeding area in the world [29], accounting for nearly 70% of the breeding habitat of this species in the world [30]. Saunders's gulls depend on *Suaeda salsa* habitats for breeding, which grow in mudflats [31]. In recent decades, some tidal marshes have been converted to aquacultural ponds, paddy fields, industrial development, and other land-use types [32]. The loss of tidal marshes shrinks the breeding habitat area of Saunders's gulls, which may lead to a decrease in Saunders's gull populations. Knowing how these conversions impact the breeding habitat of Saunders's gulls may aid in better conservation planning for this species. However, to date, long-term data on the extent to which tidal marshes have been converted into other land-use types and the potential impact of these conversions on the breeding habitat of Saunders's gulls are largely unknown.

In this study, we first generated land-use-type maps of WNRLE for four different years (1988, 2000, 2009, 2017) through interpretation of satellite images to explore how land uses change during the three decades; then, we predicted the potential breeding habitat of Saunders's gulls in each of the four years using the MaxEnt model based on the land-use map, along with other environmental variables, and analyzed the changes in the potential breeding habitat of Saunders's gulls from 1988 to 2017; finally, we proposed some suggestions for Saunders's gull conservation.

2. Methods

2.1. Study Area

The geographic location of our study area is between 121°28′09.74″E–122°00′23.92″E and 40°45′00″N–41°08′49.65″N, with a total area of 10.9×10^5 ha. It is located on the lower fluvial plain of the Liaohe River. It consists of two nature reserves—the National Wetland Nature Reserve of the Liaohe Estuary and the Provincial Wetland Nature Reserve of the Liaohe Estuary (Figure 1). The former has an area of 8.0×10^5 ha, and the latter has an area of 2.9×10^5 ha. The study area has a northern temperate, semi-humid, seasonal monsoon climate. The annual mean temperature is 8.4 °C, with a maximum of 35.2 °C in July and a minimum of −28.2 °C in January. The frozen-free days are from 167 to 174 days. The annual mean precipitation is 623.2 mm, with a maximum of 916.4 mm and a minimum of 326.6 mm. The main soil types include paddy soil, saline soil, meadow soil, and boggy soil. The major vegetation types comprise the *Phragmites australis* community and *Suaeda salsa* community. Other species include *Leymus chinensis*, *Calamagrostis epigeios*, *Xeridium sonchifolium*, *Plantago asiatica*, *Aeluropus sinensis*, *Scirpus planiculmis*, and *Typha orientalis*.

2.2. Larus Saundersi Occurrence Dataset

We obtained bird-monitoring reports from 2010 to 2017 from the Wetland Nature Reserve of the Liaohe Estuary. These reports provided a detailed inventory method for counting the number of *Larus saundersi*, which includes direct counting by telescopes and binoculars during the nonbreeding season (April) and breeding season (June) at certain sites 4–6 times each year. These observational sites were mainly located in seepweed marshes and mudflats, which are the main habitats for *Larus saundersi* to forage and breed. We compiled the records that had geographical positions at which *Larus saundersi* occurred. We obtained 122 records for *Larus saundersi* occurrence. After omitting duplicate records that were too close to each other or out of the extent of our study area, 63 out of the 122 records for *Larus saundersi* occurrence were utilized to predict its habitat suitability.

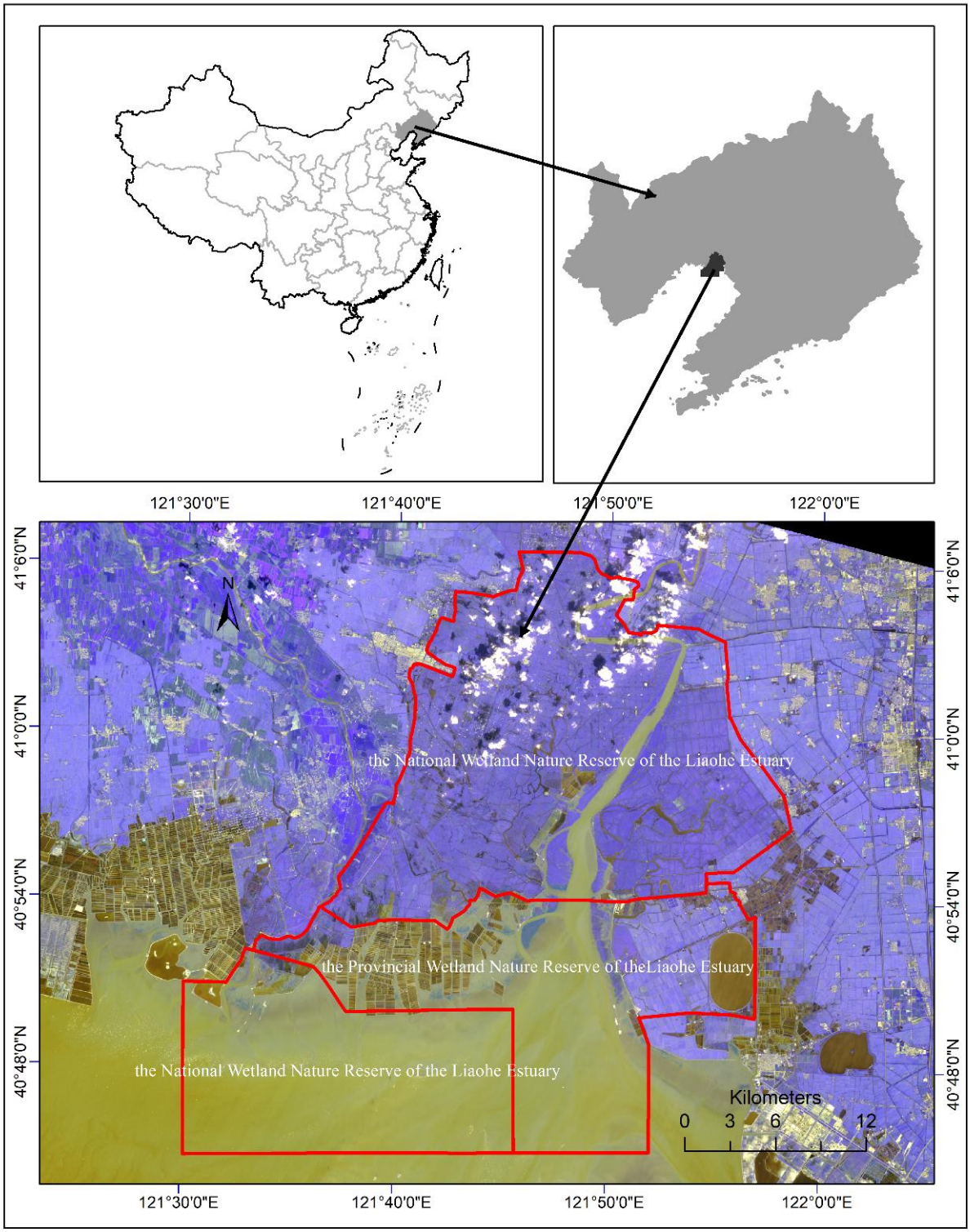

Figure 1. Geographic location of the study area. The study area consists of two nature reserves—the National Wetland Nature Reserve and the Provincial Wetland Nature Reserve of the Liaohe Estuary. The background is the RGB composite image of Landsat 8 OLI, taking band 5 as red, band 4 as green, and band 3 as blue band.

2.3. Environmental Variable Selection and Processing

Many factors may affect the spatial distribution of waterbird species, such as food and water availability, shelter conditions, and anthropogenic disturbances [33]. We chose normalized difference vegetation index (NDVI) as shelter conditions due to its indication of

vegetation cover; land use and distance to roads and artificial facilities serve as indicators of human disturbances; distance to rivers and water bodies may indicate water availability; and digital elevation model (DEM) and distance to the shoreline influence vegetation distribution and food availability.

Land-use types: We downloaded Landsat images of our study area from the USGS (https://glovis.usgs.gov/, accessed on 13 October 2017) for 1988, 2000, 2009, and 2017 to derive land-use change information. These images have a spatial resolution of 30 m. We first categorized land-use types into 9 classes—namely, non-irrigated farmland, paddy field, reed marsh, seepweed marsh, artificial facility, water body, mudflat, shrimp and crab pond, and shallow sea, according to the Chinese standard of land-use classification [34]. We projected the boundary map of the Wetland Nature Reserve of the Liaohe Estuary into the same projection as the Landsat images, and these images were cut by the boundary map to generate images within the extent of the reserve. Supervised classification was performed on the images for 1988, 2000, 2009, and 2017, and then, the classified land-use maps were corrected by visual checking. We validated the land-use classification map of 2017 by using Google Earth images according to 200 random points, resulting in an accuracy of 80.5%, which could meet our modeling requirements.

Normalized difference vegetation index (NDVI): We calculated the NDVI value in each year based on the Landsat near-infrared band and red band by using the following formula:

$$\mathrm{NDVI} = \frac{NIR - R}{NIR + R} \quad (1)$$

where *NIR* and *R* are the reflectance values of the near-infrared band and red band, respectively.

Digital elevation model (DEM): We downloaded DEM at the Resource and Environment Science and Data Center (https://www.resdc.cn, accessed on 5 December 2017). It is derived from ALOS PALSAR and has a spatial resolution of 12.5 m. We projected the DEM spatial data of the Wetland Nature Reserve of the Liaohe Estuary into the same projection as the Landsat images and resampled them to a 30 m spatial resolution.

Distance to the shoreline: We obtained a shoreline distribution map for 2017 from the Environment Science Research Institute of Liaoning Province. We first interpreted the shoreline based on Landsat images to generate shoreline distribution maps for 1988, 2000, and 2009, calculated the distances to the shoreline for 1988, 2000, 2009, and 2017, setting a cell size of 30 m, and masked these distance maps by the boundary map in the ArcGIS10.3 environment.

Distance to rivers and water bodies: We extracted water bodies from land-use maps for 1988, 2000, 2009, and 2017 and visually interpreted linear rivers based on Landsat images of the Wetland Nature Reserve of the Liaohe Estuary in 1988, 2000, 2009, and 2017. We projected the river and water body distribution maps into the same projection as Landsat images, calculated the distances to rivers and water bodies, set the resolution to 30 m, and masked the distance maps by the boundary map in the ArcGIS10.3 environment.

Distance to roads: We visually interpreted roads based on the Landsat images of the Wetland Nature Reserve of the Liaohe Estuary in 1988, 2000, 2009, and 2017 and projected the road maps into the same projection as Landsat images, calculated the distances to roads, set the cell size to 30 m, and masked the distance maps by the boundary map in the ArcGIS10.3 environment.

Distance to artificial facilities: We extracted artificial facilities from land-use maps for 1988, 2000, 2009, and 2017, calculated the distance to artificial facilities each year, set the cell size to 30 m, and masked the distance maps by the boundary map in the ArcGIS10.3 environment.

Given that many variables were spatially correlated and could cause overfitting of the prediction [35], we extracted the values of the abovementioned environmental variables for each location where *Larus saundersi* occurred. The Pearson correlation coefficient (r) was calculated in SPSS 22.0, and highly correlated environmental variables with $|r| \geq 0.8$ were

excluded [36–38]. The distance to water bodies was removed (r = 0.86), and the remaining 7 variables were used to model the occurrence probability for *Larus saundersi*.

2.4. MaxEnt Model Parameter Settings

Species distribution models (SDMs) have been important tools to assess habitat suitability in recent years [39,40]. SDMs use species records and spatial environmental factors to predict the occurrence probability of species [41]. Many SDMs have been developed using either species presence–absence data or presence-only data. For example, generalized additive models (GAMs) and general linear models (GLMs) are used for presence–absence data [42], and the genetic algorithm for ruleset production (GARP) and maximum entropy method (MaxEnt) [43] are used for presence-only data. As most species absence data are generally unavailable, SDMs for presence-only data are often used to estimate the occurrence probability of species, which is utilized to map the potential geographical distribution of the species, especially by using the MaxEnt model [44]. The MaxEnt model minimizes the relative entropy between two probability densities (environment/background and the presence data) to obtain better prediction results [45]. Since in many cases, there are a limited number of presence data available, MaxEnt model can be used, as it has been shown to perform well with a small number size [46]. Hence, the MaxEnt model is widely used to evaluate habitat suitability and predict the potential distribution of various species [43], such as *Paeonia ostii* in China [47], Oriental white stork (*Ciconia boyciana*) in central Japan [48], *Athyrium brevifrons* in northeastern China [49], and Caucasian grouse (*Lyrurus mlokosiewiczi*) in the Greater and Lesser Caucasus regions [50]. MaxEnt3.4.1 [45] was chosen in our research to predict habitat suitability for *Larus saundersi*.

In parameter setting, the number of replicate runs was set to 10, and the maximum iteration time was 500. The jackknife test and cross-validation (56 records for the training set and 7 for the testing set) were chosen, and other parameters were arranged with their default settings. Variable importance was evaluated by percent contribution. Finally, the average predicted occurrence probability of *Larus saundersi* of the 10 replicates was reclassified into 4 classes according to arbitrarily defined probability classes. We are aware of the other studies on threshold-based classifications [51–53]. These thresholds are justified depending on the goal of the study. In this study, the suitability classes were determined by the occurrence probability thresholds according to [51], with most suitable (0.6–1), suitable (0.4–0.6), less suitable (0.1–0.4), and unsuitable (0–0.1) to generate a habitat suitability map for *Larus saundersi*.

2.5. Evaluation of Model Performance

We used the area under the curve (AUC), which is the receiver operating characteristic (ROC) curve, to evaluate MaxEnt model performance [54]. AUC ranges from 0.0 to 1.0, with an AUC value $\leq$ 0.5 demonstrating the prediction is no better or worse than random; 0.5–0.7 indicating poor performance; 0.7–0.9 representing good performance; >0.9 showing exceptionally excellent performance [55,56].

2.6. Redundancy Analysis

We utilized the ordination method to explore the relationships among the changes in the suitable habitat of *Larus saundersi* and the dynamics of land uses. Ordination is often used to explore relationships between species distributions and environmental variables. It requires a species and an environmental matrix. We calculated the change rate of each habitat suitability class of *Larus saundersi* for every combination of change periods ($C_4^2 = 6$) from 1988 to 2017. The change rate of each land-use type was also calculated for the same period accordingly. We regarded the change rate of different habitat suitability classes of *Larus saundersi* as "species", the change rate of various land-use types as "environmental", and each change period as a sample. Hence, a 6 $\times$ 4 "species matrix" was established (Table S1), and a 6 $\times$ 9 environmental matrix was constructed (Table S2). To eliminate collinearity, the Pearson correlation coefficients (r) among the 9 environmental variables

were calculated in SPSS 22.0, and the highly correlated environmental variables with $|r| \geq 0.8$ were excluded [36]. Thus, AF, WB, SS, and NIF were removed, and the remaining 5 variables were used for redundancy analysis (Table 1). The analysis was performed with Canoco for Windows (Version 4.5), with variables entered by the forward selection method. Permutation tests with 499 permutations using the Monte Carlo test were utilized to evaluate the significance of variables at the 95% confidence level.

Table 1. Redundancy analysis (RDA) with the forward variable selection method. Permutation tests with 499 permutations using the Monte Carlo test were utilized to test the significance of variables at the 95% confidence level.

Variables	Variance Explained by the Variables Selected	F-Value	*p*-Value
PD	0.72	10.4	0.0020
MF	0.92	7.06	0.0700
RD	0.99	15.86	0.0580
SCP	1.00	4.79	0.1800
SW	1.00	0.00	1.0000

Notes: PD—paddy field; RD—reed marsh; SW—seepweed marsh; MF—mudflat; SCP—shrimp and crab pond.

3. Results

3.1. Land-Use Change

The supervised classification results (Figure 2) showed that reed marsh dominated the Wetland Nature Reserve of the Liaohe Estuary, ranging from 40.02% in 1988 to 38.17% in 2017. Non-irrigated farmland increased steadily, although it accounted for less than 1%. Paddy fields increased from 0.97% in 1988 to 6.40% in 2017. Shrimp and crab ponds increased steadily from 0.77% in 1988 to 6.08% in 2017. Artificial facilities increased from 0.20% in 1988 to 0.42% in 2009 and then decreased to 0.36% in 2017 (Table 2). Seepweed marsh decreased from 6.5% in 1988 to 1.07% in 2000 and then increased to 6.60% in 2017. Mudflats fluctuated between 12.71% and 21.79%.

3.2. Evaluation of MaxEnt Model Performance

The average training AUCs with 10-fold cross-validation were 0.896 ± 0.053, 0.908 ± 0.047, 0.907 ± 0.044, and 0.901 ± 0.066 for 1988, 2000, 2009, and 2017, respectively (Figure S1), showing the model's relatively good performance in predicting suitable habitat for *Larus saundersi*.

3.3. Changes in the Habitat Suitability of Larus saundersi

The predicted results of the occurrence probability of *Larus saundersi* by MaxEnt (Figure 3) were categorized into four classes in the ArcGIS 10.3 environment according to the arbitrarily defined probability classes. The most suitable and suitable habitats were mainly distributed in the southwestern part of the study area, while the less suitable habitats were on both sides of the Liaohe River (Figure 4). The area and percentage for each class are shown in Table 3. We can see that the most suitable habitat decreased from 3.69% in 1988 to 2.40% in 2009 and then increased to 2.77% in 2017. The suitable habitat decreased from 2.32% in 1988 to 1.74% in 2009 and then increased to 1.85% in 2017. The less suitable habitat fluctuated from 11.55% to 13.52%, while the unsuitable habitat increased from 80.42% in 1988 to 83.04% in 2017.

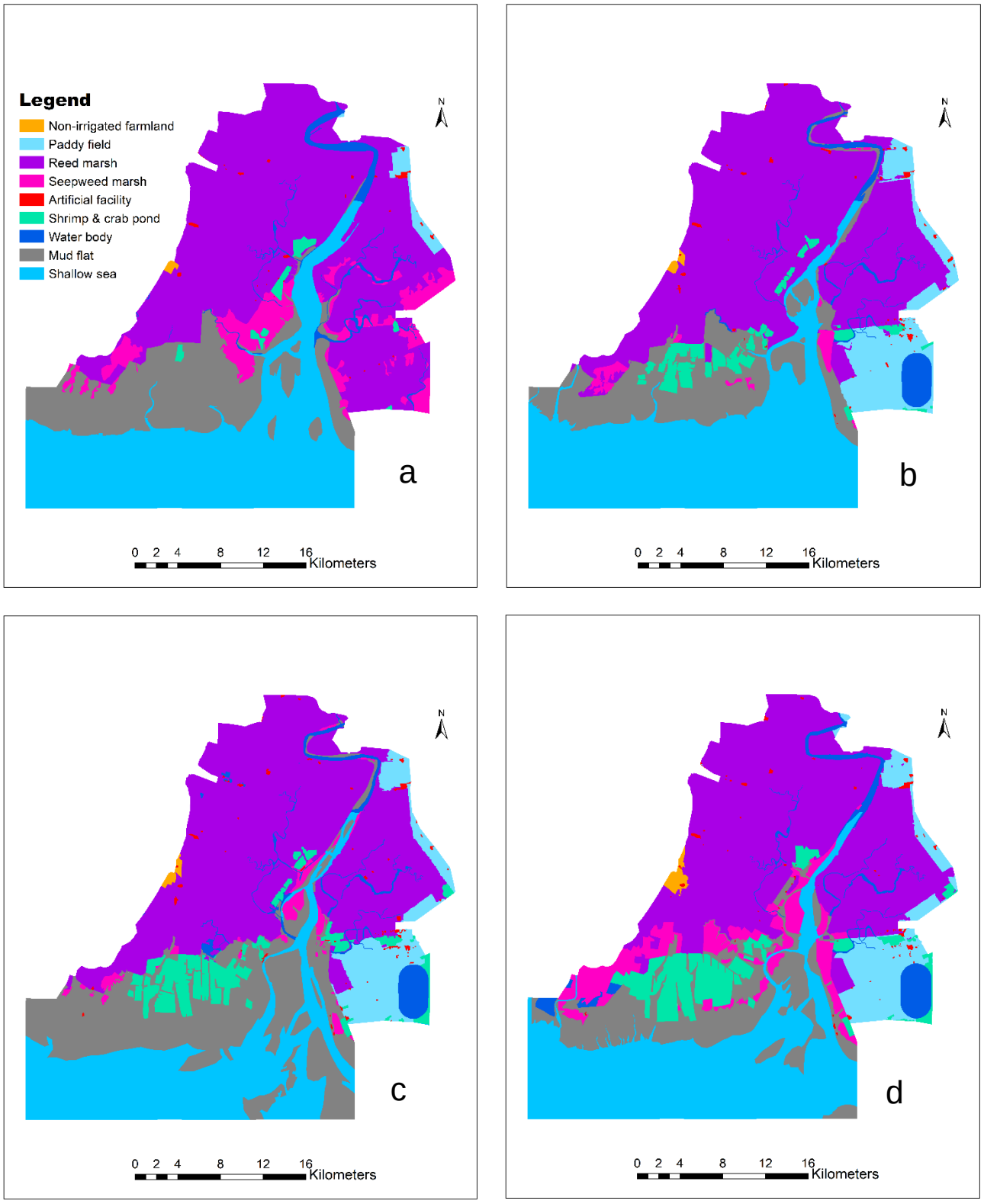

Figure 2. Land-use map of the Wetland Nature Reserve of the Liaohe Estuary: (**a**) 1988, (**b**) 2000, (**c**) 2009, and (**d**) 2017. These maps were generated by supervised classification on the Landsat images for 1988, 2000, 2009, and 2017, respectively, and classification errors were corrected by visual checking, resulting in overall accuracies greater than 80%.

Table 2. Area (ha) and percentage (%) of each land-use type in 1988, 2000, 2009, and 2017.

Land-Use Type	1988		2000		2009		2017	
	Area (ha)	Percent (%)	Area (ha)	Percent (%)	Area (ha)	Percent (%)	Area (ha)	Percent (%)
Non-irrigated farmland	98.66	0.10	148.66	0.15	200.07	0.20	399.50	0.40
Paddy field	964.55	0.97	6794.52	6.75	6358.55	6.37	6399.99	6.40
Reed marsh	43,948.33	40.02	41,716.19	41.42	40,753.22	40.82	38,153.68	38.17
Seepweed marsh	6490.27	6.50	1081.05	1.07	1537.82	1.54	6600.79	6.60
Artificial facility	195.09	0.20	347.72	0.35	420.32	0.42	359.43	0.36
Water body	2068.55	2.07	2636.09	2.62	2915.49	2.92	3323.22	3.32
Mudflat	16,577.82	16.60	14,777.34	14.67	21,754.75	21.79	12,704.79	12.71
Shrimp and crab pond	773.47	0.77	2982.01	2.96	5289.31	5.30	6078.73	6.08
Shallow sea	28,708.90	28.76	30,226.96	30.01	20,598.39	20.63	25,941.58	25.95

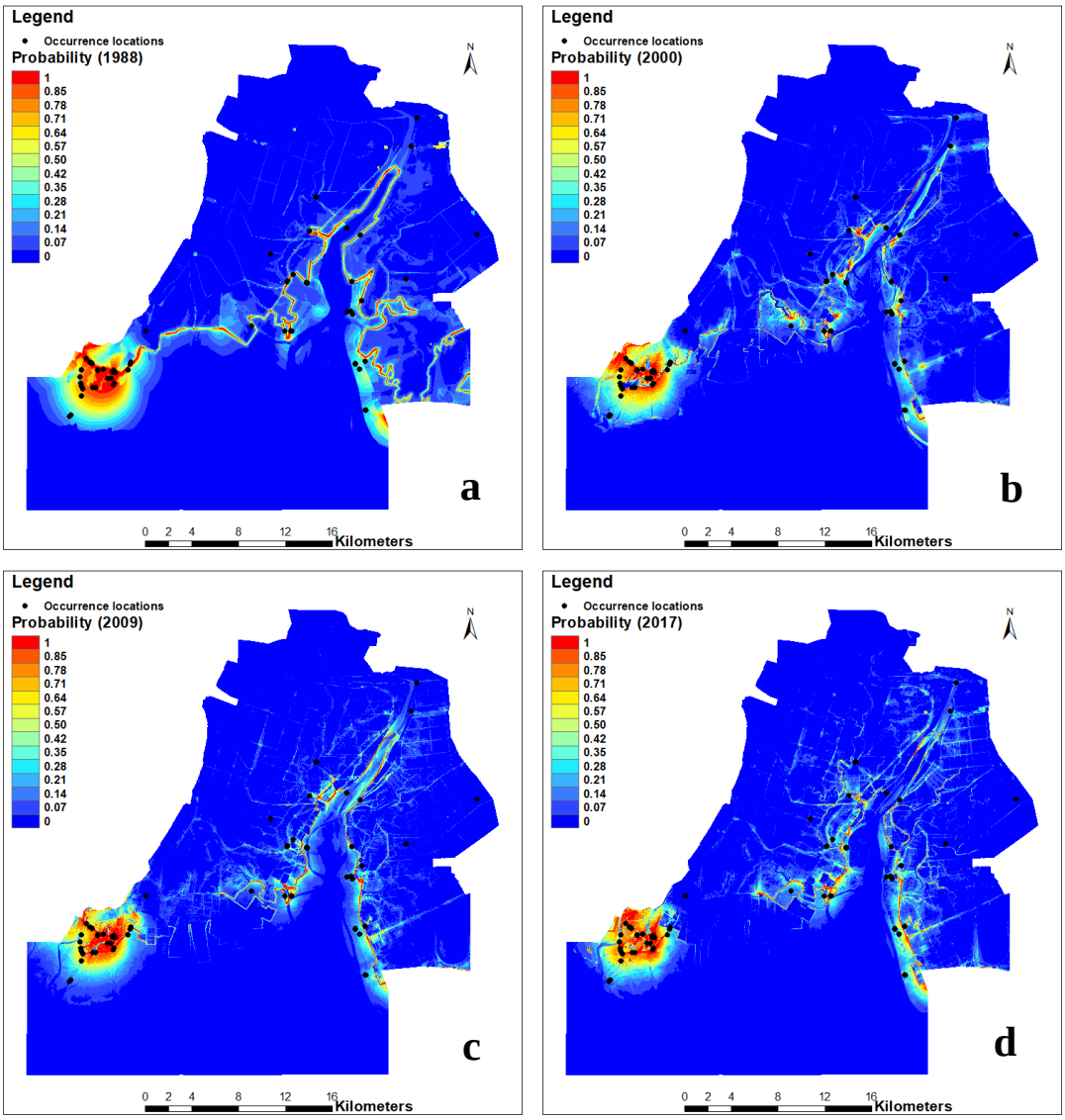

Figure 3. Occurrence probability of *Larus saundersi* predicted by the MaxEnt model in the Wetland Nature Reserve of the Liaohe Estuary: (**a**) 1988, (**b**) 2000, (**c**) 2009, and (**d**) 2017. The black dots are the occurrence locations of *Larus saundersi*.

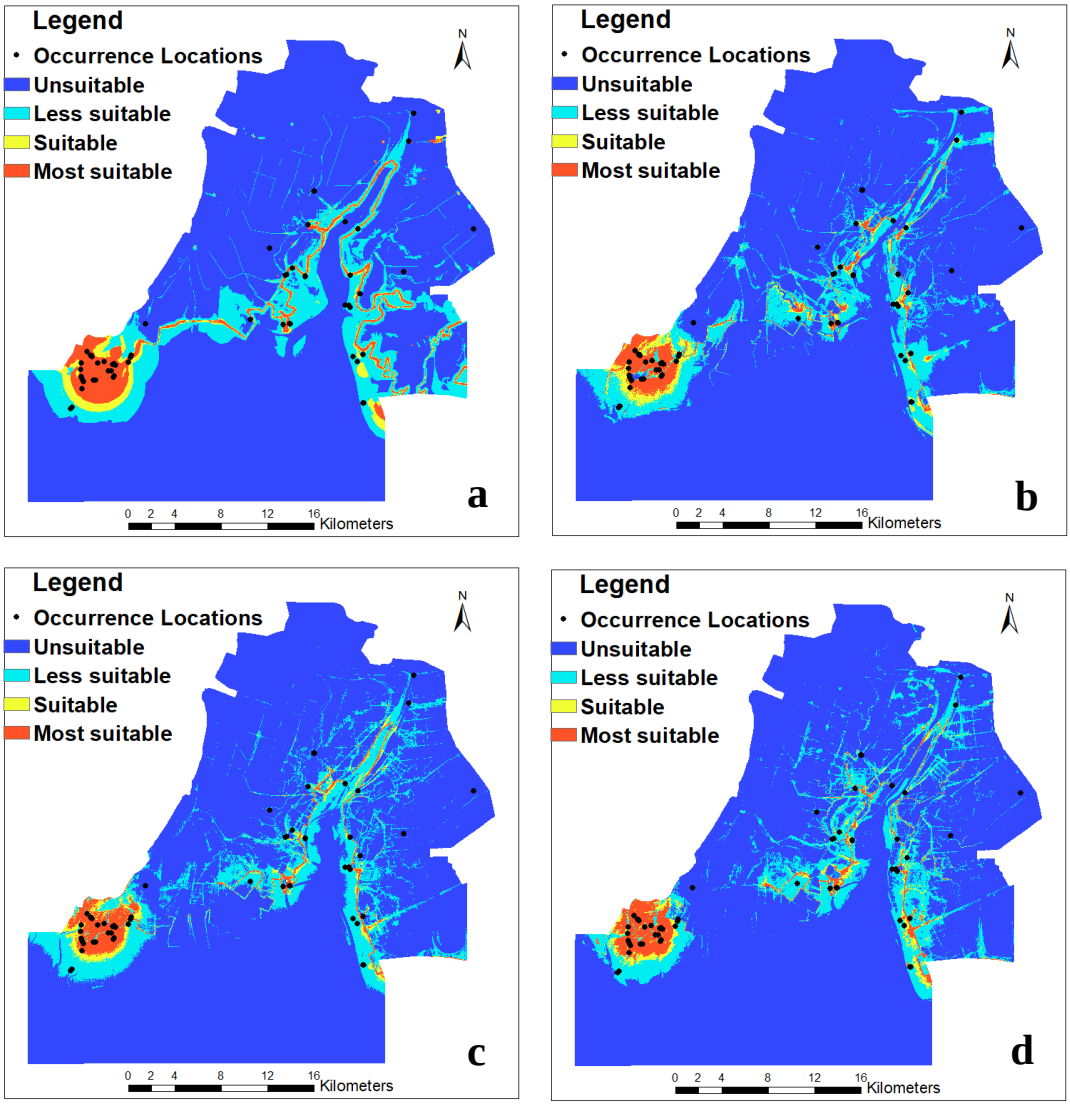

Figure 4. Habitat suitability distribution maps of *Larus saundersi* in the Wetland Nature Reserve of the Liaohe Estuary: (**a**) 1988, (**b**) 2000, (**c**) 2009, and (**d**) 2017. Several methods have been suggested to categorize the results based on the thresholds [51–53]. These thresholds are justified depending on the goal of the study. In this study, the suitability classes were determined by the occurrence probability thresholds according to [51], with most suitable (0.6–1), suitable (0.4–0.6), less suitable (0.1–0.4), and unsuitable (0–0.1).

Table 3. Area and percentage of each suitable class for *Larus saundersi* distribution in 1988, 2000, 2009, and 2017.

Suitable Class	1988		2000		2009		2017	
	Area (ha)	Percent (%)	Area (ha)	Percent (%)	Area (ha)	Percent (%)	Area (ha)	Percent (%)
Unsuitable	80,280.09	80.42	83,799.09	83.94	83,073.96	83.22	82,895.13	83.04
Less suitable	13,492.80	13.52	11,530.44	11.55	12,620.16	12.64	12,320.46	12.34
Suitable	2316.42	2.32	2033.46	2.04	1733.94	1.74	1848.96	1.85
Most suitable	3686.94	3.69	2465.55	2.47	2400.48	2.40	2763.99	2.77
Total	99,828.54	100.00	99,828.54	100.00	99,828.54	100.00	99,828.54	100.00

3.4. Factors Influencing the Habitat Suitability of Larus saundersi

The jackknife tests showed the relative contribution of each environmental variable to the *Larus saundersi* distribution predicted by the MaxEnt model (Figure S2, Table S4).

We found that land use, distance to the coastline, distance to artificial facilities, distance to rivers, distance to roads, and the NDVI had certain degrees of impact on the *Larus saundersi* distribution. The contributions of land use ranged from 16.4% to 40.3%, distance to the coastline from 34.7% to 48.0%, distance to artificial facilities from 5.9% to 11.1%, distance to rivers from 5.5% to 11.0%, distance to roads from 3.9% to 12.5%, and the NDVI from 0.3% to 6.3% (Table S4).

In addition, the response curves (Figure S3) showed that the breeding habitat of *Larus saundersi* is mainly located in mudflats and seepweed marshes, where NDVI ranged from −0.05 to 0.05. We also found a high occurrence probability of Saunders's gulls where the elevation was less than 0.95 m and the distance to the shoreline was within 10 m. The occurrence probability of Saunders's gulls reached the highest when the distance to roads was 8674 m.

3.5. The Impact of Land-Use Change on the Habitat Suitability of Larus saundersi

The RDA results showed that the first canonical axis explained 78.9% of the variance in the habitat suitability of *Larus saundersi*. The first and second canonical axes together explained 99.2% of the habitat suitability of *Larus saundersi*. The most suitable habitat for *Larus saundersi* had a positive relationship with the change in SW. The unsuitable habitat for *Larus saundersi* had a positive relationship with changes in PD, SCP, and MF (Figure 5).

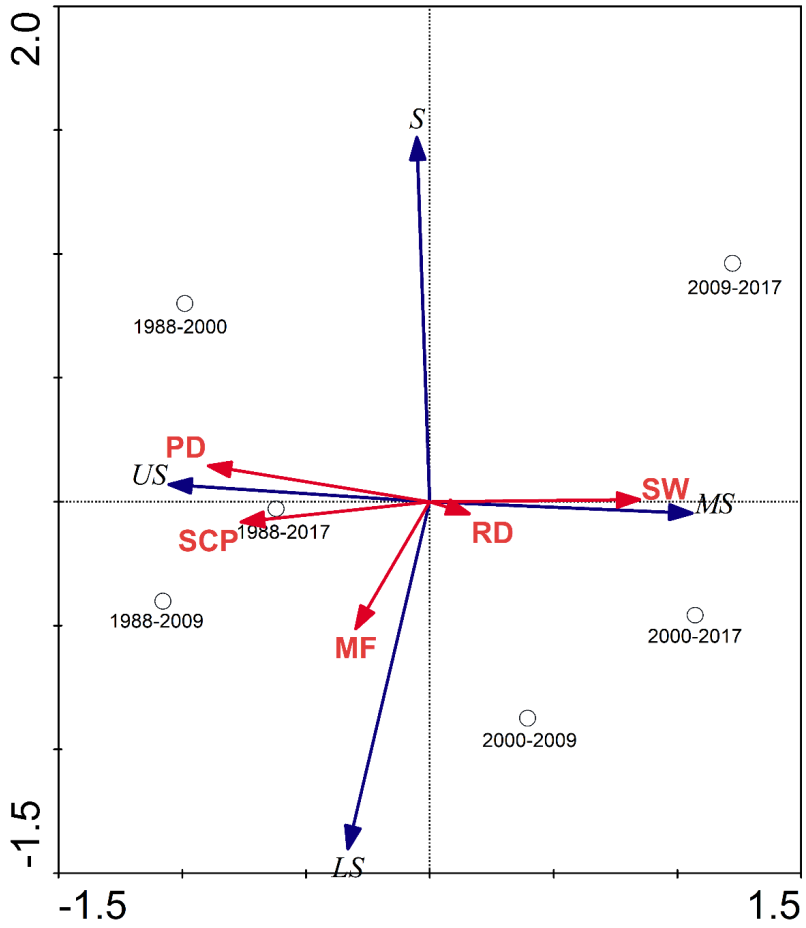

Figure 5. Ordination diagram of RDA with samples (change periods), species (the change rate of different habitat suitability classes of *Larus saundersi*), and environmental variables (the change rate of various land-use types), taking the first canonical factor as the *x*-axis and the second canonical factor as the *y*-axis. The habitat suitability classes were represented as US-unsuitable, LS-less suitable, S-suitable, and MS-most suitable. Changes in land-use types such as PD-paddy field, RD-reed marsh, SW-seepweed marsh, MF-mudflat, and SCP-shrimp and crab pond.

4. Discussion

4.1. Factors Influencing the Habitat Suitability of Larus saundersi

A previous report showed that factors that affect the breeding habitat of Saunders's gulls include vegetation cover, anthropogenic disturbance intensity, water availability, and food abundance [33]. In our study, we chose land use/cover as an indicator for food abundance, the NDVI for vegetation cover, the DEM and distance to the coastline as indirect indicators for food abundance because they influence the distribution of vegetation, distance to rivers and water bodies for water availability, and distance to roads and constructed facilities for human disturbance intensity. The simulation results from the MaxEnt model indicated that the spatial distribution of the breeding habitat for Saunders's gulls could be well simulated using these spatial environmental variables. The jackknife test (Figure S2, Table S4) suggested that land use, distance to the coastline, distance to artificial facilities, distance to roads and rivers, and the NDVI are the major factors affecting the breeding habitat for Saunders's gulls.

Our results showed that the breeding habitat of *Larus saundersi* is mainly located in mudflats and seepweed marshes (Figure 4 and Figure S3). Our results are in line with field observations of previous researchers [31,57] and are comparable to the habitat of slender-billed gulls [58] and black-headed gulls [59]. Saunders's gulls often perch on near-sea mudflats at night and find food on mudflats, current ditches, and seepweed marsh wetlands because the favorite foods for Saunders's gulls such as *Bullacta exarate*, *Nereis succinea*, *Synechogobius hasta*, *Macrophthalmus dilatatum*, and *Helice tientsinensis* [60] are largely distributed there [61].

We found that a high occurrence probability of Saunders's gulls was observed where the NDVI ranged from −0.05 to 0.05 (Figure S3). A low NDVI is consistent with the habitat requirements of Saunders's gulls [62]. They usually nest above the upper rim of the tidal zone where short and sparse *Suaeda salsa* grow to protect their nests from seawater flushing even when high tides occur [31]. The short and sparse *Suaeda salsa* vegetation generally has a low NDVI. This kind of habitat type is also favored by other bird species, such as black terns (*Chlidonias niger*) [63] and DuPont's lark [64].

We also found a high occurrence probability of Saunders's gulls where the elevation was less than 0.95 m and the distance to the shoreline was within 10 m (Figure S3). This is because the *Suaeda salsa* wetland, a nesting area for Saunders's gulls, is distributed in a near-sea mudflat. In areas with relatively higher DEMs, dense *Phragmites australis* grows, which is unfavorable for Saunders's gulls [57].

Anthropogenic disturbances, such as coastal development and recreational activities [65], have negative impacts on bird habitats [39]. Our results indicated that the occurrence probability of Saunders's gulls reaches the highest when the distance to roads is 8674 m (Figure S3). If using 0.4 as the threshold between suitable and unsuitable habitat according to Remya et al. (2015), we could determine that the impacting distance from roads and artificial facilities on the breeding habitat selection of Saunders's gulls is approximately 2000 m and 2200 m, respectively. The influence of roads on breeding habitat selection of Saunders's gulls is comparable to that of less black-backed gulls, which select habitat 2 km offshore, to avoid human disturbances [66].

4.2. Land-Use Change and Habitat Suitability Dynamics of Larus saundersi

Land-use change-induced loss of wetlands has seriously threatened the habitat of waterfowl [8]. Our results indicated that paddy fields and aquacultural ponds have increased steadily. Artificial facilities first increased and then decreased, while marshland decreased steadily. The increase in artificial facilities was mainly attributed to ecotourism development during 1988–2009. The increase in ponds was mainly due to the reclamation of mudflat wetlands for aquacultural development. The increase in paddy fields from 1988 to 2000 was mainly due to the reclamation of wetlands for agricultural development. The reclamation of wetlands is common in coastal areas of China. For example, in the Yellow River Delta, one of the three breeding places of *Larus saundersi* in China, 1.34% of wetlands

covered by *Suaeda salsa* were transformed into reservoirs and ponds, and 24.71% were covered with *Phragmites australis* into dry farmland from 1976 to 2016 [67]. Marshes are the most degraded wetlands in China [68].

The transformation of wetlands to other land-use types may have great impacts on bird habitat. Previous studies have demonstrated that land-use/cover change is the main driver of bird habitat loss [69], and long-term coastal reclamation has greatly undermined coastal wetlands' functions as waterbird habitats [32]. In our study, the favorable habitat (most suitable plus suitable) of Saunders's gulls decreased by 1868.94 ha during 1988-2009 (Table 2). This is partly due to the conversion of wetlands to artificial facilities and aquacultural ponds. The construction of roads, dams, and other facilities would have changed the hydrokinetic conditions and increased the sediment accretion rate [70], which would limit the establishment of *Suaeda salsa*, resulting in a massive shrinkage of *Suaeda salsa* vegetation [71].

The reclamation of wetlands to aquacultural ponds directly destroyed the habitat of Saunders's gulls. Our results were consistent with recent studies in the Yancheng National Nature Reserve, where the loss of *Larus saundersi* habitat is largely attributed to the widespread expansion of aquaculture [28,62].

In addition, the "red beach (*Suaeda salsa*)" landscape has beautiful scenery that attracts thousands of people to visit. Ecotourism significantly contributes to the local economy. However, the frequent presence of tourists has reduced the density of waterbirds, which, in turn, has increased the density of crabs, which are lethal herbivores, driving the further degradation of coastal red beaches [72].

4.3. Implications for Effective Conservation of Larus saundersi

Most biosphere reserves currently face conflicts between biodiversity conservation and economic development [73]. In wetland nature reserves, the conservation of wetland bird habitats has become a global conservation priority [72]. The MaxEnt model can better predict the spatial distribution of the breeding habitat suitability of Saunders's gulls. The dynamic change information for the habitat of Saunders's gulls, both spatially and temporally, in this study can be used to conduct future conservation planning in our study area and other related regions. We found that the suitable breeding habitat of Saunders's gulls was largely located in the southwestern part of the reserve, suitability decreased during 1988–2009 and had an increasing trend during 2009–2017 (Figure 4), and Saunders's gulls favored mudflats and seepweed marshes (Figure S3, Table S3). This part of the reserve should be strictly conserved. However, the Wetland Nature Reserve of the Liaohe Estuary is managed by two different reserves—the National Wetland Nature Reserve of the Liaohe Estuary and the Provincial Wetland Nature Reserve of the Liaohe Estuary (Figure 1). The national nature reserve has stricter regulations for nature conservation than the provincial nature reserve. Hence, we suggest that the managers of the two reserves take equally strict measures to conserve the habitat of Saunders's gulls by employing efficient coordination and cooperation, especially for seepweed marshes. Indeed, China has taken "beautiful China" and "ecological civilization" as national strategies since 2012, and the Wetland Nature Reserve of the Liaohe Estuary has been categorized as an "ecological red line" area [74]. All these strategies will guarantee the effective conservation of the breeding habitat of Saunders's gulls.

In addition, habitat management is an important approach to maintaining bird habitat [75,76]. Saunders's gulls have special requirements for choosing their nesting sites that include lower and sparse *Suaeda salsa* vegetation above the upper rim of the tidal zone. The height and density of *Suaeda salsa* and the surface water level have a direct influence on the successful breeding of Saunders's gulls. Reserve managers have accumulated successful practices for conserving the breeding habitat of Saunders's gulls. They have cut higher *Suaeda salsa* vegetation (>90 cm) to reduce the height of *Suaeda salsa* and have dug ditches and built sluice gates to control the surface water level. Burning is also recommended to

create suitable vegetation cover for *Suaeda salsa*. All these practices have maintained or even enlarged the extent of the breeding habitat of Saunders's gulls [30].

5. Limitations

In our study, we only explored the impacts of land-use changes and human disturbances on the breeding habitat suitability of Saunders's gulls during 1988–2017. In fact, other factors may also have certain degrees of impact, such as climate change. Previous results have indicated that climate change may affect the habitat distribution of bird species [77]. The possible effect of climate change needs to be considered as well, but its effect is unlikely to be as considerable as land-use change. Hence, the changing trend of the suitable breeding habitat of Saunders's gulls during 1988–2017 is robust in our study and could be used to make conservation planning for Saunders's gulls. Quantifying the impact of climate change on the breeding habitat suitability of Saunders's gulls is our future research focus.

6. Conclusions

Knowledge of breeding habitat changes of Saunders's gulls could aid in management strategies for this "vulnerable" species. Our results demonstrated that human-induced changes in seepweed marshes and coastline position are the main factors influencing the potential breeding habitat of Saunders's gulls. The potential breeding habitat of Saunders's gulls decreased steadily during 1988–2009 due to the development of aquaculture and tourism and had an increasing trend during 2009–2017 with the implementation of "beautiful China" and "ecological civilization" national strategies. Efficient coordination and cooperation between the National Wetland Nature Reserve and the Provincial Wetland Nature Reserve of the Liaohe Estuary could guarantee the effective conservation of the breeding habitat of Saunders's gulls, especially in the seepweed marshes. In addition, the implementation of habitat management practices could enlarge the extent of the breeding habitat of Saunders's gulls.

Supplementary Materials: The following are available online at: https://www.mdpi.com/article/10.3390/rs14030552/s1, Figure S1: ROC curves for evaluating the performance of the MaxEnt model. a-1988, b-2000, c-2009, and d-2017; Figure S2: Importance of environmental variables to Larus saundersi distribution by using jackknife analysis. a-1988, b-2000, c-2009, and d-2017; Figure S3: Response curves of selected environmental variables to predicted probability contributions using 2009 as an example; Table S1: Change rate (%) of different habitat suitability classes of Larus saundersi during various change periods; Table S2: Change rate (%) of different land-use types during various change periods; Table S3: Area and percentage of every land-use type out of each habitat suitability class of Larus saundersi in different years; Table S4: Relative contributions of environmental variables to the Larus saundersi distribution predicted by the Maxent model.

Author Contributions: Investigation, Y.H.; project administration, M.L.; resources, Y.L. and J.L.; writing—original draft preparation, Y.C.; manuscript revision, C.C. All authors have read and agreed to the published version of the manuscript.

Funding: This research was supported by the National Key Research and Development Project of China (2016YFC0500401) and the Strategic Priority Research Program of the Chinese Academy of Sciences (XDA23070103).

Data Availability Statement: Available on request.

Acknowledgments: We thank the anonymous reviewers for their very helpful suggestions to improve the manuscript.

Conflicts of Interest: The authors declare no competing interests.

References

1. Xiao, D.; Deng, L.; Kim, D.-G.; Huang, C.; Tian, K. Carbon budgets of wetland ecosystems in China. *Glob. Chang. Biol.* **2019**, *25*, 2061–2076. [CrossRef] [PubMed]

2. Sutton-Grier, A.; Howard, J. Coastal wetlands are the best marine carbon sink for climate mitigation. *Front. Ecol. Environ.* **2018**, *16*, 73–74. [CrossRef]
3. Hopkinson, C.S.; Cai, W.-J.; Hu, X. Carbon sequestration in wetland dominated coastal systems—A global sink of rapidly diminishing magnitude. *Curr. Opin. Environ. Sustain.* **2012**, *4*, 186–194. [CrossRef]
4. Xiu, L.; Yan, C.; Li, X.; Qian, D.; Feng, K. Changes in wetlands and surrounding land cover in a desert area under the influences of human and climatic factors: A case study of the Hongjian Nur region. *Ecol. Indic.* **2019**, *101*, 261–273. [CrossRef]
5. Dixon, M.J.R.; Loh, J.; Davidson, N.C.; Beltrame, C.; Freeman, R.; Walpole, M. Tracking global change in ecosystem area: The Wetland Extent Trends index. *Biol. Conserv.* **2016**, *193*, 27–35. [CrossRef]
6. Copeland, H.E.; Tessman, S.A.; Girvetz, E.H.; Roberts, L.; Enquist, C.; Orabona, A.; Patla, S.; Kiesecker, J. A geospatial assessment on the distribution, condition, and vulnerability of Wyoming's wetlands. *Ecol. Indic.* **2010**, *10*, 869–879. [CrossRef]
7. Hu, S.; Niu, Z.; Chen, Y.; Li, L.; Zhang, H. Global wetlands: Potential distribution, wetland loss, and status. *Sci. Total Environ.* **2017**, *586*, 319–327. [CrossRef]
8. Bai, Q.; China Coastal Waterbird Census Group; Chen, J.; Chen, Z.; Dong, G.; Dong, J.; Dong, W.; Fu, V.W.K.; Han, Y.; Lu, G.; et al. Identification of coastal wetlands of international importance for waterbirds: A review of China Coastal Waterbird Surveys 2005–2013. *Avian Res.* **2015**, *6*, 12. [CrossRef]
9. Fardila, D.; Kelly, L.T.; Moore, J.L.; McCarthy, M.A. A systematic review reveals changes in where and how we have studied habitat loss and fragmentation over 20years. *Biol. Conserv.* **2017**, *212*, 130–138. [CrossRef]
10. Yu, H.; Li, L.; Zhu, W.; Piao, D.; Cui, G.; Kim, M.; Jeon, S.W.; Woo-Kyun Lee, W.-K. Drought monitoring of the wetland in the Tumen River Basin between 1991 and 2016 using Landsat TM/ETM+. *Int. J. Remote Sens.* **2019**, *40*, 1445–1459. [CrossRef]
11. Cao, C.X.; Zhao, J.; Gong, P.; Ma, G.R.; Bao, D.M.; Tian, K.; Tian, R.; Niu, Z.G.; Zhang, H.; Xu, M.; et al. Wetland changes and droughts in southwestern China. *Geomat. Nat. Hazards Risk* **2011**, *3*, 79–95. [CrossRef]
12. Heintzman, L.J.; McIntyre, N.E. Quantifying the effects of projected urban growth on connectivity among wetlands in the Great Plains (USA). *Landsc. Urban Plan.* **2019**, *186*, 1–12. [CrossRef]
13. Mondal, B.; Dolui, G.; Pramanik, M.; Maity, S.; Biswas, S.S.; Pal, R. Urban expansion and wetland shrinkage estimation using a GIS-based model in the East Kolkata Wetland, India. *Ecol. Indic.* **2017**, *83*, 62–73. [CrossRef]
14. Murray, N.J.; Clemens, R.S.; Phinn, S.R.; Possingham, H.P.; Fuller, R.A. Tracking the rapid loss of tidal wetlands in the Yellow Sea. *Front. Ecol. Environ.* **2014**, *12*, 267–272. [CrossRef]
15. Davis, C.L.; Miller, D.A.W.; Campbell Grant, E.H.; Halstead, B.J.; Kleeman, P.M.; Walls, S.C.; Barichivich, W.J. Linking variability in climate to wetland habitat suitability: Is it possible to forecast regional responses from simple climate measures? *Wetl. Ecol. Manag.* **2019**, *27*, 39–53. [CrossRef]
16. Fu, B.; Pollino, C.A.; Cuddy, S.M.; Andrews, F. Assessing climate change impacts on wetlands in a flow regulated catchment: A case study in the Macquarie Marshes, Australia. *J. Environ. Manag.* **2015**, *157*, 127–138. [CrossRef] [PubMed]
17. Schuerch, M.; Spencer, T.; Temmerman, S.; Kirwan, M.L.; Wolff, C.; Lincke, D.; McOwen, C.J.; Pickering, M.D.; Reef, R.; Vafeidis, A.T.; et al. Future response of global coastal wetlands to sea-level rise. *Nature* **2018**, *561*, 231–234. [CrossRef]
18. Cellone, F.; Carol, E.; Tosi, L. Coastal erosion and loss of wetlands in the middle Río de la Plata estuary (Argentina). *Appl. Geogr.* **2016**, *76*, 37–48. [CrossRef]
19. Eppink, F.V.; van den Bergh, J.C.J.M.; Rietveld, P. Modelling biodiversity and land use: Urban growth, agriculture and nature in a wetland area. *Ecol. Econ.* **2004**, *51*, 201–216. [CrossRef]
20. Harrison, P.A.; Berry, P.M.; Henriques, C.; Holman, I.P. Impacts of socio-economic and climate change scenarios on wetlands: Linking water resource and biodiversity meta-models. *Clim. Chang.* **2008**, *90*, 113–139. [CrossRef]
21. Sica, Y.V.; Quintana, R.D.; Radeloff, V.C.; Gavier-Pizarro, G.I. Wetland loss due to land use change in the Lower Paraná River Delta, Argentina. *Sci. Total Environ.* **2016**, *568*, 967–978. [CrossRef] [PubMed]
22. Mao, D.; Luo, L.; Wang, Z.; Wilson, M.C.; Zeng, Y.; Wu, B.; Wu, J. Conversions between natural wetlands and farmland in China: A multiscale geospatial analysis. *Sci. Total Environ.* **2018**, *634*, 550–560. [CrossRef] [PubMed]
23. Zheng, X.J.; Sun, P.; Zhu, W.H.; Xu, Z.; Fu, J.; Man, W.D.; Li, H.L.; Zhang, J.; Qin, L. Landscape dynamics and driving forces of wetlands in the Tumen River Basin of China over the past 50 years. *Landsc. Ecol. Eng.* **2017**, *13*, 237–250. [CrossRef]
24. Fickas, K.C.; Cohen, W.B.; Yang, Z. Landsat-based monitoring of annual wetland change in the Willamette Valley of Oregon, USA from 1972 to 2012. *Wetl. Ecol. Manag.* **2016**, *24*, 73–92. [CrossRef]
25. Song, K.; Wang, Z.; Du, J.; Liu, L.; Zeng, L.; Ren, C. Wetland Degradation: Its Driving Forces and Environmental Impacts in the Sanjiang Plain, China. *Environ. Manag.* **2014**, *54*, 255–271. [CrossRef]
26. Xia, S.; Yu, X.; Millington, S.; Liu, Y.; Jia, Y.; Wang, L.; Hou, X.; Jiang, L. Identifying priority sites and gaps for the conservation of migratory waterbirds in China's coastal wetlands. *Biol. Conserv.* **2017**, *210*, 72–82. [CrossRef]
27. Konoff, M.D.; Royle, J.A. Modeling wetland change along the United States Atlantic Coast. *Ecol. Model.* **2004**, *177*, 41–59. [CrossRef]
28. Jiang, H.X.; Hou, Y.Q.; Chu, G.Z.; Qian, F.W.; Wang, H.; Zhang, G.G.; Zheng, G.M. Breeding population dynamics and habitat transition of Saunders's Gull Larus saundersi in Yancheng National Nature Reserve, China. *Bird Conserv. Int.* **2010**, *20*, 13–24. [CrossRef]
29. Yang, F.; Li, Y.; Chao, X.; Yang, Y.; Li, X.; Yunfeng, L. Biodiversity and Developing Strategy of Shuantaihekou Nature Reserve. *J. Liaoning For. Sci. Technol.* **1998**, *5*, 15–20.

30. Zhou, J.; Li, D.; Ren, J.; Liu, D. The Dynamic Changes, Preservation and Restoration of Larus saundersi 's Breeding Habitat in Liao Estuary Wetland. *China Gard. For.* **2017**, *33*, 123–128. (In Chinese)
31. Yan, L.; Lv, J. Investugation on the breeding stutus of Saunders's Gulls. *J. Shandong For. Sci. Technol.* 1994; 26–28. (In Chinese)
32. Ma, T.; Li, X.; Bai, J.; Cui, B. Habitat modification in relation to coastal reclamation and its impacts on waterbirds along China's coast. *Glob. Ecol. Conserv.* **2019**, *17*, e00585. [CrossRef]
33. Liu, C.Y.; Qing, Z.S.; Jiang, H.X.; Li, X.F.; Na, X.D.; Wen, Z.F. Remote sensing monitoring on dynamic of nesting habitats of Saunders′s Gul l Larus saundersi. *Acta Ecol. Sin.* **2009**, *29*, 4285–4294.
34. *GB/T 21010-2017*; National Standards for Land Use Classification. Standardization Administration of the P. R. China: Beijing, China, 2017.
35. Yan, H.; Feng, L.; Zhao, Y.; Feng, L.; Zhu, C.; Qu, Y.; Wang, H. Predicting the potential distribution of an invasive species, *Erigeron canadensis* L., in China with a maximum entropy model. *Glob. Ecol. Conserv.* **2020**, *21*, e00822. [CrossRef]
36. Yang, X.-Q.; Kushwaha, S.P.S.; Saran, S.; Xu, J.; Roy, P.S. Maxent modeling for predicting the potential distribution of medicinal plant, *Justicia adhatoda* L. in Lesser Himalayan foothills. *Ecol. Eng.* **2013**, *51*, 83–87. [CrossRef]
37. Di Pasquale, G.; Saracino, A.; Bosso, L.; Russo, D.; Moroni, A.; Bonanomi, G.; Allevato, E. Coastal Pine-Oak Glacial Refugia in the Mediterranean Basin: A Biogeographic Approach Based on Charcoal Analysis and Spatial Modelling. *Forests* **2020**, *11*, 673. [CrossRef]
38. Du, Z.; He, Y.; Wang, H.; Wang, C.; Duan, Y. Potential geographical distribution and habitat shift of the genus Ammopiptanthus in China under current and future climate change based on the MaxEnt model. *J. Arid Environ.* **2021**, *184*, 104328. [CrossRef]
39. Almalki, M.; Alrashidi, M.; O'Connell, M.J.; Shobrak, M.; Szekely, T. Modelling the distribution of wetland birds on the red sea coast in the kingdom of saudi arabia. *Appl. Ecol. Environ. Res.* **2015**, *13*, 67–84.
40. Morán-Ordóñez, A.; Lahoz-Monfort, J.J.; Elith, J.; Wintle, B.A. Evaluating 318 continental-scale species distribution models over a 60-year prediction horizon: What factors influence the reliability of predictions? *Glob. Ecol. Biogeogr.* **2017**, *26*, 371–384. [CrossRef]
41. Fournier, A.; Barbet-Massin, M.; Rome, Q.; Courchamp, F. Predicting species distribution combining multi-scale drivers. *Glob. Ecol. Conserv.* **2017**, *12*, 215–226. [CrossRef]
42. Meynard, C.N.; Quinn, J.F. Predicting species distributions: A critical comparison of the most common statistical models using artificial species. *J. Biogeogr.* **2007**, *34*, 1455–1469. [CrossRef]
43. Phillips, S.J.; Anderson, R.P.; Schapire, R.E. Maximum entropy modeling of species geographic distributions. *Ecol. Model.* **2006**, *190*, 231–259. [CrossRef]
44. Elith, J.; Phillips, S.J.; Hastie, T.; Dudík, M.; Chee, Y.E.; Yates, C.J. A statistical explanation of MaxEnt for ecologists. *Divers. Distrib.* **2011**, *17*, 43–57. [CrossRef]
45. Phillips, S.J.; Anderson, R.P.; Dudík, M.; Schapire, R.E.; Blair, M.E. Opening the black box: An open-source release of Maxent. *Ecography* **2017**, *40*, 887–893. [CrossRef]
46. Na, X.; Zhou, H.; Zang, S.; Wu, C.; Li, W.; Li, M. Maximum Entropy modeling for habitat suitability assessment of Red-crowned crane. *Ecol. Indic.* **2018**, *91*, 439–446. [CrossRef]
47. Zhang, K.; Zhang, Y.; Zhou, C.; Meng, J.; Sun, J.; Zhou, T.; Tao, J. Impact of climate factors on future distributions of Paeonia ostii across China estimated by MaxEnt. *Ecol. Inform.* **2019**, *50*, 62–67. [CrossRef]
48. Yamada, Y.; Itagawa, S.; Yoshida, T.; Fukushima, M.; Ishii, J.; Nishigaki, M.; Ichinose, T. Predicting the distribution of released Oriental White Stork (*Ciconia boyciana*) in central Japan. *Ecol. Res.* **2019**, *34*, 277–285. [CrossRef]
49. Li, Y.; Cao, W.; He, X.; Chen, W.; Sheng, X. Prediction of Suitable Habitat for Lycophytes and Ferns in Northeast China: A Case Study on *Athyrium brevifrons*. *Chin. Geogr. Sci.* **2019**, *20*, 1011–1023. [CrossRef]
50. Habibzadeh, N.; Storch, I.; Ludwig, T. Differential habitat associations in peripheral populations of threatened species: The case of the Caucasian grouse. *Ecol. Res.* **2019**, *34*, 309–319. [CrossRef]
51. Remya, K.; Ramachandran, A.; Jayakumar, S. Predicting the current and future suitable habitat distribution of Myristica dactyloides Gaertn. using MaxEnt model in the Eastern Ghats, India. *Ecol. Eng.* **2015**, *82*, 184–188. [CrossRef]
52. Liu, C.; Berry, P.M.; Dawson, T.P.; Pearson, R.G. Selecting thresholds of occurrence in the prediction of species distributions. *Ecography* **2005**, *28*, 385–393. [CrossRef]
53. Narouei-Khandan, H.A.; Worner, S.P.; Viljanen, S.L.H.; van Bruggen, A.H.C.; Jones, E.E. Projecting the suitability of global and local habitats for myrtle rust (*Austropuccinia psidii*) using model consensus. *Plant Pathol.* **2020**, *69*, 17–27. [CrossRef]
54. Merow, C.; Smith, M.J.; Silander, J.A. A practical guide to MaxEnt for modeling species' distributions: What it does, and why inputs and settings matter. *Ecography* **2013**, *36*, 1058–1069. [CrossRef]
55. West, A.M.; Kumar, S.; Brown, C.S.; Stohlgren, T.J.; Bromberg, J. Field validation of an invasive species Maxent model. *Ecol. Inform.* **2016**, *36*, 126–134. [CrossRef]
56. Zhang, Y.; Tang, J.; Ren, G.; Zhao, K.; Wang, X. Global potential distribution prediction of Xanthium italicum based on Maxent model. *Sci. Rep.* **2021**, *11*, 16545. [CrossRef]
57. Liu, H. Propagation Study of Saundersus Gull at Shandong Yellow River Delta. *Shandong For. Sci. Technol.* **2015**, *5*, 86–87,103.
58. Baaloudj, A.; Bouzid, A.; Nedjah, R.; Samraoui, F.; Samizaoui, B. Distribution and breeding of the slender-billed gull chroicocephalus genei, common tern sterna hirundo and little tern sternula albifrons in algeria. *Rev. Ecol.-Terre Vie* **2018**, *73*, 385–395.
59. Dai, S.; Feng, D.L.; Xu, B. Monitoring potential geographical distribution of four wild bird species in China. *Environ. Earth Sci.* **2016**, *75*, 10. [CrossRef]

60. Wang, X.; Jiang, H.X.; Zhang, Y.N.; Chen, L.X.; Song, C.Z.; Li, Y.X. Diet composition of Saunders's Gull (*Larus saundersi*) determined using stable isotope analysis at the Shuangtaihekou National Nature Reserve, China. *Acta Ecol. Sin.* **2017**, *37*, 1796–1804.
61. Yoon, J.; Yoon, H.-J.; Go, B.-G.; Joo, E.-J.; Park, S.-R. Tide associated incubation and foraging behaviour of Saunders's Gulls *Larus saundersi*. *Ardea* **2013**, *101*, 99–104. [CrossRef]
62. Liu, C.; Jiang, H.; Hou, Y.; Zhang, S.; Su, L.; Li, X.; Pan, X.; Wen, Z. Habitat Changes for Breeding Waterbirds in Yancheng National Nature Reserve, China: A Remote Sensing Study. *Wetlands* **2010**, *30*, 879–888. [CrossRef]
63. Wyman, K.E.; Cuthbert, F.J. Black tern (*Chlidonias niger*) breeding site abandonment in U.S. Great Lakes coastal wetlands is predicted by historical abundance and patterns of emergent vegetation. *Wetl. Ecol. Manag.* **2017**, *25*, 583–596. [CrossRef]
64. Anton, A.G.; Garza, V.; Justribo, J.H.; Traba, J. Factors affecting Dupont's lark distribution and range regression in Spain. *PLoS ONE* **2019**, *14*, 22.
65. Yorio, P.; Petracci, P.; Garcia Borboroglu, P. Current status of the threatened Olrog's Gull Larus atlanticus: Global population, breeding distribution and threats. *Bird Conserv. Int.* **2013**, *23*, 477–486. [CrossRef]
66. Warwick-Evans, V.C.; Atkinson, P.W.; Robinson, L.A.; Green, J.A. Predictive Modelling to Identify Near-Shore, Fine-Scale Seabird Distributions during the Breeding Season. *PLoS ONE* **2016**, *11*, 17. [CrossRef]
67. Cong, P.; Chen, K.; Qu, L.; Han, J. Dynamic Changes in the Wetland Landscape Pattern of the Yellow River Delta from 1976 to 2016 Based on Satellite Data. *Chin. Geogr. Sci.* **2019**, *29*, 372–381. [CrossRef]
68. Xing, L.; Niu, Z. Mapping and analyzing China's wetlands using MODIS time series data. *Wetl. Ecol. Manag.* **2019**, *27*, 693–710. [CrossRef]
69. Brambilla, M.; Gustin, M.; Vitulano, S.; Falco, R.; Bergero, V.; Negri, I.; Bogliani, G.; Celada, C. Sixty years of habitat decline: Impact of land-cover changes in northern Italy on the decreasing ortolan bunting *Emberiza hortulana*. *Reg. Environ. Change* **2017**, *17*, 323–333. [CrossRef]
70. Jiang, H.-X.; Chu, G.-Z.; Hou, Y.-Q.; Qian, F.-W.; Wang, H.; Zhang, G.-G.; Zheng, G.-M. Spatiotemporal variation of nesting sites of the Saunders' s gull Larus saundersi. *Acta Zool. Sin.* **2008**, *54*, 191–200.
71. Wang, Y.; Liu, R.; Gao, H.; Bai, J.; Ling, M. Degeneration Mechanism Research of Suaeda Heteroptera Wetland of the Shuangtaizi Estuary National Nature Reserve in China. *Procedia Environ. Sci.* **2010**, *2*, 1157–1162. [CrossRef]
72. Lu, W.; Xiao, J.; Lei, W.; Du, J.; Li, Z.; Cong, P.; Hou, W.; Zhang, J.; Chen, L.; Zhang, Y.; et al. Human activities accelerated the degradation of saline seepweed red beaches by amplifying top-down and bottom-up forces. *Ecosphere* **2018**, *9*, e02352. [CrossRef]
73. Ma, Z.; Li, B.; Li, W.; Han, N.; Chen, J.; Watkinson, A.R. Conflicts between biodiversity conservation and development in a biosphere reserve. *J. Appl. Ecol.* **2009**, *46*, 527–535. [CrossRef]
74. Wang, X.; Kuang, F.; Tan, K.; Ma, Z. Population trends, threats, and conservation recommendations for waterbirds in China. *Avian Res.* **2018**, *9*, 14. [CrossRef]
75. Gilbert, G.; Tyler, G.A.; Dunn, C.J.; Smith, K.W. Nesting habitat selection by bitterns Botaurus stellaris in Britain and the implications for wetland management. *Biol. Conserv.* **2005**, *124*, 547–553. [CrossRef]
76. Ma, Z.; Cai, Y.; Li, B.; Chen, J. Managing Wetland Habitats for Waterbirds: An International Perspective. *Wetlands* **2010**, *30*, 15–27. [CrossRef]
77. Bateman, B.L.; Pidgeon, A.M.; Radeloff, V.C.; Flather, C.H.; VanDerWal, J.; Akakaya, H.R.; Thogmartin, W.E.; Albright, T.P.; Vavrus, S.J.; Heglund, P.J. Potential breeding distributions of US birds predicted with both short-term variability and long-term average climate data. *Ecol. Appl.* **2016**, *26*, 2718–2729. [CrossRef]